

Dipole Moments of Perturbed Poly(vinyl chloride), Poly(vinyl bromide), and Poly(*p*-chlorostyrene)

Wayne L. Mattice* and Anthony C. Lloyd

Department of Chemistry, Louisiana State University, Baton Rouge, Louisiana 70803-1804.
Received March 25, 1986

ABSTRACT: Recent work (*Macromolecules* 1984, 17, 625; 1985, 18, 2236) has shown that the mean square dipole moment, $\langle \mu^2 \rangle$, of model chains with a finite number of bonds, n , may depend on excluded volume even if $\langle \mathbf{r} \cdot \boldsymbol{\mu} \rangle_0 = 0$. The end-to-end vector and dipole moment vector are denoted by \mathbf{r} and $\boldsymbol{\mu}$, respectively, angle brackets denote the statistical mechanical average of the enclosed term, and the subscript zero denotes the ensemble that is unperturbed by long-range interactions. The present work demonstrates that (1) conclusions reached earlier for model chains also apply to realistic chains, (2) effects seen with finite chains may survive in extremely long chains, (3) the limit at large n for $(\alpha_r^2 - 1)/(\alpha_\mu^2 - 1)$ provides little information about the effect of excluded volume on the dipole moment of infinitely long chains, and (4) an alternative relationship between α_μ^2 and α_r^2 may provide useful information on the relationship of $\langle \mu^2 \rangle$ and $\langle \mu^2 \rangle_0$ for long chains. The chains examined are rotational isomeric state models for poly(vinyl chloride), poly(vinyl bromide), and poly(*p*-chlorostyrene). The probability for a meso diad, p_m , is 0, 0.5, or 1 and n is 100-400 in the chains considered. The results show that α_μ^2 has a significant dependence on α_r^2 for long chains in which $p_m = 0$. A much weaker dependence is seen when $p_m = 0.5$ or 1.

In the early 1970s Nagai and Ishikawa¹ and also Doi² studied the mean square dipole moment, $\langle \mu^2 \rangle$, in chains perturbed by excluded volume. Their conclusions are summarized by the equation

$$\alpha_\mu^2 - 1 = x(\alpha_r^2 - 1) \quad (1)$$

$$x = \langle \mathbf{r} \cdot \boldsymbol{\mu} \rangle_0^2 [\langle r^2 \rangle_0 \langle \mu^2 \rangle_0]^{-1} \quad (2)$$

where \mathbf{r} and $\boldsymbol{\mu}$ denote the end-to-end and dipole moment vectors, respectively, r^2 is the square of the end-to-end distance, angle brackets denote the statistical mechanical average of the enclosed term, the subscript zero denotes the ensemble that is unperturbed by long-range interaction, $\alpha_r^2 = \langle r^2 \rangle / \langle r^2 \rangle_0$, and $\alpha_\mu^2 = \langle \mu^2 \rangle / \langle \mu^2 \rangle_0$. Equations 1 and 2 were derived for chains so large that the number of bonds, n , can be considered to be infinite. Two important conclusions follow from these equations.¹ First, α_μ^2 must be 1 if $\langle \mathbf{r} \cdot \boldsymbol{\mu} \rangle_0 = 0$. This conclusion has broad application because the great majority of chains likely to be of interest have $\langle \mathbf{r} \cdot \boldsymbol{\mu} \rangle_0 = 0$. The mean square dipole moment for such polymers should not be affected by expansion of the chain. Second, chains for which $\langle \mathbf{r} \cdot \boldsymbol{\mu} \rangle_0 \neq 0$ must have $\alpha_\mu^2 > 1$ if $\alpha_r^2 > 1$. The possibility that $\alpha_\mu^2 < 1 < \alpha_r^2$ is eliminated because x cannot be negative.

Recent simulations of the behavior of model chains with finite n find behavior that is in conflict with both predictions.^{3,4} There are two simple model chains that exhibit the supposedly forbidden behavior $\alpha_\mu^2 < 1 < \alpha_r^2$ and a larger number of model chains that have $\langle \mathbf{r} \cdot \boldsymbol{\mu} \rangle_0 = 0$ and $\langle \mu^2 \rangle$ that change upon the imposition of excluded volume.

The following considerations are sufficient for construction of a simple model chain for which $\alpha_\mu^2 < 1 < \alpha_r^2$. Select the bond angle so that the largest end-to-end distance is obtained in the planar trans configuration. Short-range interactions should provide no penalty for the occupancy of trans placements by consecutive bonds, but they must also allow other rotational states that produce smaller end-to-end distances. (The widely accepted rotational isomeric state model for polyethylene has these characteristics.⁵) Group dipole moment vectors are then assigned to the units in the chain in a manner that yields a net dipole moment of zero for subchains in which all internal bonds occupy trans rotational states. (When the fully extended chain defines the xy plane, the group dipole moment vectors might be parallel to the z axis and al-

ternate in direction.) If expansion is accompanied by an increase in the probability for occupancy of trans placements by consecutive bonds, the chain will then have $\langle \mathbf{r} \cdot \boldsymbol{\mu} \rangle_0 = 0$ and $\alpha_\mu^2 < 1 < \alpha_r^2$. This conclusion is supported by the simulation of a model chain with these characteristics.³

It remains to be established whether the results with the model chains conclusively demonstrate that eq 1 and 2 do not describe the behavior of *real* polymers of extremely high molecular weight. For that reason we have examined realistic rotational isomeric state models of poly(vinyl chloride) (PVC), poly(vinyl bromide) (PVB), and poly(*p*-chlorostyrene) (PCIS) over a range of n that permits an extrapolation to the behavior of extremely long chains. The stereochemical compositions considered were $p_m = 0$, 0.5, and 1, where p_m denotes the probability of a meso placement. Chains with $p_m = 0.5$ have behavior that is well described by eq 1 and 2, but large departures from such behavior are seen in racemic chains. An intermediate situation is encountered in some meso chains.

Simulations

Rotational Isomeric State Models. The rotational isomeric state model employed for unperturbed PVC is the one described by Mark.⁶ The C-C-C angle is 112°, gauche states occur at $\pm 120^\circ$ from the trans state, and the statistical weights for first- and second-order interactions are $\eta = 4.2$, $\tau = 0.45$, $\omega = \omega' = 0.032$, and $\omega'' = 0.071$. The group dipole moment is taken to be parallel to the C-Cl bond. The rotational isomeric state model for unperturbed PVB differs from that for PVC in that the C-C-C angles alternate between 112° and 114°, with the larger angle at C-CH₂-C, and the statistical weights are $\eta = 1.29$, $\tau = 0.43$, $\omega = 0.015$, $\omega' = 0.034$, and $\omega'' = 0.0024$.⁷ The configurational statistics for unperturbed PCIS are adequately described by a rotational isomeric state model developed for unperturbed polystyrene.⁸ Suitable statistical weights at 300 K are $\eta = 1.56$, $\tau = 0$, and $\omega = \omega' = \omega'' = 0.045$.⁹ The C-C-C angles alternate between 112° and 114°, as was the case in PVB. We have chosen to place the gauche states at $\pm 120^\circ$ from the trans state, as was done for PVC and PVB.

Ensemble Averages. Samples of between 40 000 and 100 000 representative unperturbed chains were generated with a priori and conditional probabilities extracted from the configuration partition function using standard methods.¹⁰ When p_m was 0.5, the unperturbed ensemble

Table I
Simulation of $\langle \mu^2 \rangle$ in Perturbed Poly(vinyl bromide) with $p_m = 0^a$

r^*/l	$n = 100$		$n = 200$		$n = 300$		$n = 400$	
	α_r^2	α_μ^2	α_r^2	α_μ^2	α_r^2	α_μ^2	α_r^2	α_μ^2
0.6	1.018	1.003	1.036	1.004	1.047	1.007	1.055	1.005
0.7	1.049	1.018	1.079	1.024	1.093	1.030	1.104	1.020
0.8	1.062	1.020	1.102	1.024	1.121	1.035	1.136	1.018
0.9	1.080	1.022	1.132	1.028	1.157	1.042	1.176	1.025
1.0	1.094	1.026	1.155	1.032	1.187	1.046	1.212	1.035
1.2	1.143	1.047	1.221	1.056	1.264	1.079	1.304	1.066
1.6	1.167	1.050	1.265	1.059	1.322	1.079	1.378	1.072
1.9	1.185	1.054	1.299	1.061	1.364	1.085	1.424	1.073

^aThe ratio of the diameter of the hard sphere to the length of a C-C bond is denoted by r^*/l .

Table II
Simulation of $\langle \mu^2 \rangle$ in Perturbed Poly(vinyl bromide) with $p_m = 0.5^a$

r^*/l	$n = 100$		$n = 200$		$n = 300$		$n = 400$	
	α_r^2	α_μ^2	α_r^2	α_μ^2	α_r^2	α_μ^2	α_r^2	α_μ^2
0.7	1.020	1.001	1.041	1.001	1.057	1.002	1.068	1.008
0.8	1.028	1.002	1.057	1.001	1.088	1.005	1.093	1.009
0.9	1.036	1.003	1.074	1.002	1.100	1.008	1.116	1.011
1.1	1.051	1.005	1.105	1.004	1.138	1.008	1.160	1.021
1.5	1.080	1.005	1.155	1.006	1.206	1.009	1.231	1.017
1.9	1.106	1.007	1.201	1.008	1.262	1.010	1.296	1.016
2.3	1.133	1.009	1.242	1.008	1.310	1.015	1.363	1.019
2.7	1.163	1.011	1.287	1.010	1.361	1.014	1.426	1.026

^aThe ratio of the diameter of the hard sphere to the length of a C-C bond is denoted by r^*/l .

contained equal numbers of configurations for each of 200 stereochemical sequences. The stereochemical sequences were generated with the assumption that the microstructure was Bernoullian. Summation of r^2 and μ^2 for all chains, followed by division by the number of chains, yields $\langle r^2 \rangle_0$ and $\langle \mu^2 \rangle_0$, respectively.

Excluded volume was introduced by a minor variation of the method employed in the simulations of the model chains.^{3,4} A hard sphere with radius r^* is centered on alternate chain atoms. A chain survives the imposition of excluded volume if there are no overlaps of hard spheres connected by seven or more bonds. Averages of r^2 and μ^2 for the surviving chains produce $\langle r^2 \rangle$ and $\langle \mu^2 \rangle$, respectively, and the expansion factors are $\alpha_r^2 = \langle r^2 \rangle / \langle r^2 \rangle_0$ and $\alpha_\mu^2 = \langle \mu^2 \rangle / \langle \mu^2 \rangle_0$. The method used here differs from the one employed in the simulation of the model chains^{3,4} only in that hard spheres are assigned to alternate chain atoms instead of every chain atom. Both methods yield the same dependence of α_μ^2 on α_r^2 , and the present study of the response of the optical anisotropy to chain expansion.¹¹

Results

Poly(vinyl bromide). Illustrative data for PVB with $p_m = 0.0$ and 0.5 are presented in Tables I and II, respectively. The expansion factors for the end-to-end distance have a reasonable dependence on r^*/l and on n . In each table, the α_r^2 increase as r^*/l increases at constant n , and they also increase with chain length at constant r^*/l . The α_μ^2 listed in Tables I and II are not randomly clustered about 1, as might have been expected if the true α_μ^2 were exactly 1. Instead the α_μ^2 are uniformly greater than 1. Different sets of r^*/l were used at $p_m = 0.0$ and 0.5 so that comparable ranges of α_r^2 would be covered in each table. Even though the ranges for α_r^2 are comparable, significantly different ranges are covered by the α_μ^2 in the two tables. The larger α_μ^2 are found in the racemic PVB chain. When n is in the range 100–400, $\langle \mu^2 \rangle$ for PVB chains responds to chain expansion, and it does so in a manner that depends on p_m .

The data in Tables I and II are processed in Figures 1 and 2 in a manner that permits estimation of the behavior

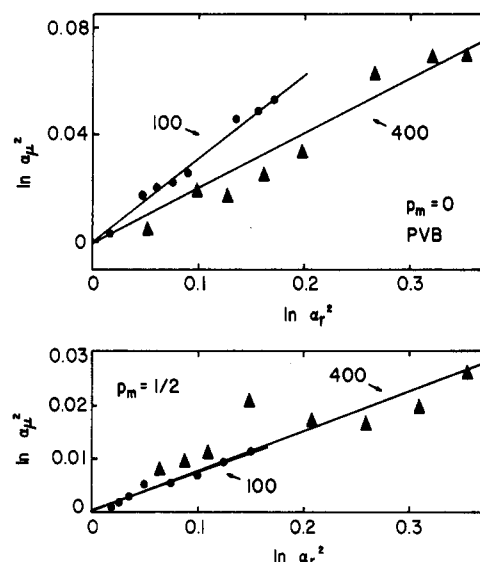


Figure 1. Relationship between $\ln \alpha_\mu^2$ and $\ln \alpha_r^2$ for PVB chains with 100 and 400 backbone bonds and stereochemical compositions characterized by $p_m = 0$ (top panel) and 0.5 (bottom panel).

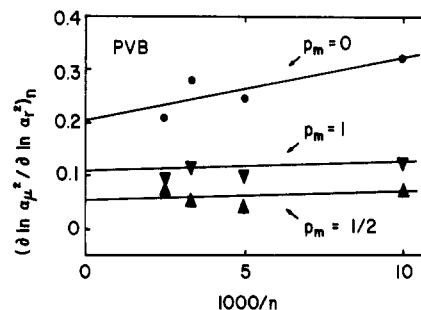


Figure 2. Estimation of a for large PVB chains.

of much longer chains. Circles in Figure 1 show $\ln \alpha_\mu^2$ as a function of $\ln \alpha_r^2$ for PVB when $n = 100$ and $p_m = 0.0$ (top panel) or $p_m = 0.5$ (bottom panel). Straight lines with slopes 0.32 and 0.07 provide a reasonable description of

Table III
 $(\partial \ln \alpha_\mu^2 / \partial \ln \alpha_r^2)_\infty$ for Three Monosubstituted Vinyl Polymers

polymer	$p_m = 0$	$p_m = 1/2$	$p_m = 1$
PVB	0.20	0.05	0.11
PVC	0.31	0.02	0.03
PCIS	0.23	0.01	0.07

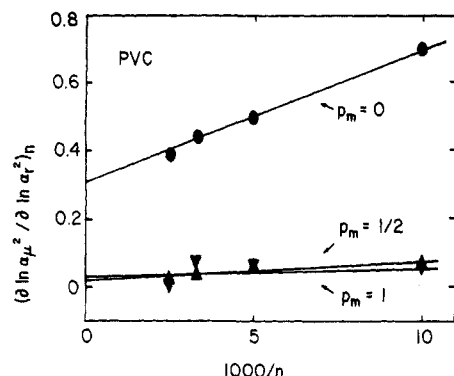


Figure 3. Estimation of a for large PVC chains.

the data. Therefore a concise summary of the second and third columns of Tables I and II is

$$\alpha_\mu^2 = (\alpha_r^2)^a \quad (3)$$

with $a = 0.32$ or 0.07 , respectively.

The triangles in Figure 1 present the dependence of α_μ^2 on α_r^2 when $n = 400$. The data plotted are from the last two columns of Tables I and II. When $p_m = 0$, there is a weaker dependence of α_μ^2 on α_r^2 in the longer chain. The best straight line through the triangles in the upper panel has a slope of 0.21. The increased scatter at $n = 400$ makes it more difficult to ascertain whether the increase in n produces a change in slope in the lower panel, where $p_m = 0.5$. The empirical relationship in eq 3 provides a useful summary of the data.

The behavior of PVB chains with $n > 400$ can be estimated by an empirical extrapolation of the a for chains with $n = 100, 200, 300$, and 400 . Figure 2 depicts the slopes of the straight lines in Figure 1, as well as the slopes of the lines that describe the data for $n = 200$ and 300 in Tables I and II and equivalent data for PVB chains with $p_m = 1$. Linear extrapolation to $1/n = 0$ yields an intercept of 0.05 for the PVB with $p_m = 0.5$. The scatter in the four upward pointing triangles is sufficient so that this intercept may not be significantly different from zero. The exponent a in eq 3 is extremely close to zero, and might actually be zero, for PVB of high molecular weight when $p_m = 0.5$.

A rather different situation is found with racemic PVB. Extrapolation of the results for chains with n of 100–400 shows that the excluded volume effect on $\langle \mu^2 \rangle$ persists to extremely large n . The best straight line through the four circles yields an intercept of 0.20. An intermediate situation is seen with the meso polymer. The best straight line yields an intercept of 0.11. The intercepts of the three lines in Figure 2 are collected in Table III.

Poly(vinyl chloride). Data for PVC were treated in the same manner as that described above for PVB. Figure 3 depicts the data for PVC in a manner similar to that employed for PVB in Figure 2. The qualitative features are much the same in both figures. The excluded volume effect on $\langle \mu^2 \rangle$ persists to extremely high n if $p_m = 0$, and a much smaller effect is seen if p_m is 0.5 or 1. There are a few differences in the two figures. The racemic PVC chain exhibits less scatter than the racemic PVB, and racemic PVC has the higher intercept. Figure 3 suggests

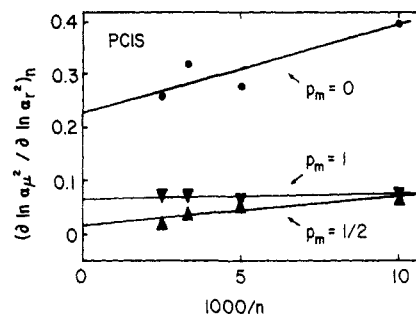


Figure 4. Estimation of a for large PCIS chains.

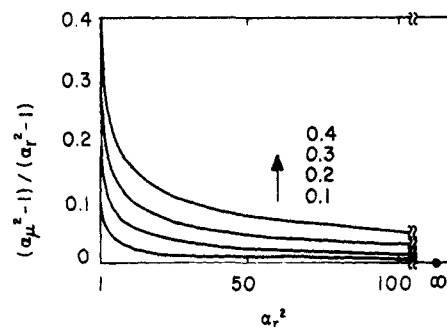


Figure 5. $(\alpha_\mu^2 - 1)/(\alpha_r^2 - 1)$ vs. α_r^2 when $\alpha_\mu^2 = (\alpha_r^2)^a$ and $a = 0.1, 0.2, 0.3$, and 0.4 .

large PVC chains with p_m of 0.5 or 1 should have α_μ^2 that are virtually independent of α_r^2 .

Poly(*p*-chlorostyrene). Figure 4 depicts a vs. $1/n$ for racemic, intermediate, and meso PCIS chains. The behavior is similar in all important aspects to that seen with PVB in Figure 2. Estimates of a for very long chains are collected in Table III.

Discussion

Informative Relationship between α_μ^2 and α_r^2 . As written, eq 1 and 2 imply that α_μ^2 for an infinitely long chain can be calculated from α_r^2 and x . The information content in these equations is better understood if the simple rearrangement⁴

$$\lim_{n \rightarrow \infty} (\alpha_\mu^2 - 1)/(\alpha_r^2 - 1) = x \quad (4)$$

is interpreted in light of the behavior of the model chain that Mattice and Carpenter have shown to have $\alpha_\mu^2 < 1 < \alpha_r^2$.³ When r^*/l is 2.7, that model chain has α_μ^2 of 0.90, 0.88, 0.86, and 0.84 at n of 100, 200, 300, and 400, respectively. The α_r^2 for these chains are 1.22, 1.37, 1.45, and 1.55, respectively. With no additional information, one can safely state that x in eq 4 must be zero. The argument is as follows: The values of α_μ^2 decrease as n increases, but α_μ^2 can never fall below zero because it is the ratio of two positive numbers. Therefore the asymptotic limit for the numerator, $\alpha_\mu^2 - 1$, cannot be more negative than -1 . On the other hand, α_r^2 increases without limit as n increases. Since the denominator increases without limit while the numerator remains finite, $(\alpha_\mu^2 - 1)/(\alpha_r^2 - 1)$ must be zero even if the limit for α_μ^2 is also zero! Mansfield¹² has recently provided a more rigorous demonstration that x is zero for the model chain described by Mattice and Carpenter.

Even if eq 4 is correct, it provides little useful information on the manner in which $\langle \mu^2 \rangle$ responds to chain expansion. The fact that x is zero does not imply that $\alpha_\mu^2 = 1$ for chains of either finite or infinite n if those chains are perturbed by excluded volume. It merely states that

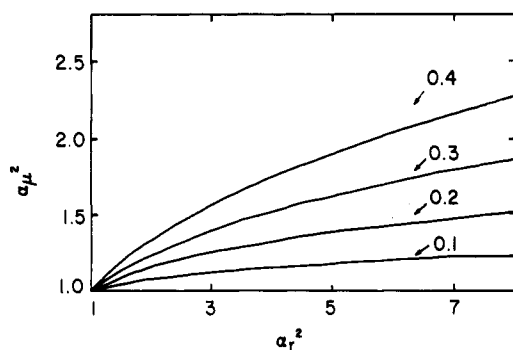


Figure 6. α_μ^2 vs. α_r^2 when $\alpha_\mu^2 = (\alpha_r^2)^a$ and $a = 0.1, 0.2, 0.3$, and 0.4 .

α_μ^2 either remains finite or approaches infinity more slowly than does α_r^2 .

With the aid of two figures, we now contrast the information conveyed by eq 3 and 4. Figure 5 depicts $(\alpha_\mu^2 - 1)/(\alpha_r^2 - 1)$ as a function of α_r^2 when α_μ^2 is given by eq 3 with a of 0.1, 0.2, 0.3, or 0.4. Certain real chains with large n can be expected to have a in this range, as shown in Table III. All four curves in Figure 5 have zero as their limit as α_r^2 becomes infinite. Since α_r^2 increases without limit as n becomes infinite, all four curves are in harmony with eq 4 if x is zero. In Figure 6, α_μ^2 is shown as a function of α_r^2 for the same four values of a . In graphic fashion, Figures 5 and 6 show that α_μ^2 can increase without limit as α_r^2 increases, even though the limit for $(\alpha_\mu^2 - 1)/(\alpha_r^2 - 1)$ may be zero. In the event that a is negative, α_μ^2 will decrease as α_r^2 increases, but the chain will still obey the limit specified in eq 4 if x is zero.

Racemic Chains. The Introduction describes a simple model chain for which $\alpha_\mu^2 < 1 < \alpha_r^2$. Let the model chain define the xy plane when all internal bonds occupy trans states. Then the dipole moment vectors associated with the bonds are perpendicular to this plane, and they alternate in direction as one proceeds along the chain. There is a perfect cancellation of the dipole moment vectors for adjacent bonds. The polar side chains occur on alternate

sides of the plane defined by the backbone when a racemic PVB, PVC, or PCIS chain adopts a configuration in which all bonds occupy trans states. However, the three racemic vinyl polymers have $1 < \alpha_\mu^2 < \alpha_r^2$ rather than $\alpha_\mu^2 < 1 < \alpha_r^2$. Racemic PVB, PVC, and PCIS chains have a behavior different from the simple model chain. The dipole moment vector for each polar side chain in the racemic vinyl polymers has a component that lies in the plane of the fully extended chain. All of the components in the plane of the backbone are parallel when gauche placements are absent. It is the parallel alignment of the in-plane components in the fully extended racemic vinyl polymers that is responsible for $1 < \alpha_\mu^2 < \alpha_r^2$.

The mean square dipole moment for some, but not all, vinyl polymers should be solvent-dependent. The absence of a useful theory that relates α_μ^2 to α_r^2 makes it difficult to obtain $\langle \mu^2 \rangle_0$ from a measured $\langle \mu^2 \rangle$.

Acknowledgment. We thank Professor Mansfield for kindly providing a preprint of ref 12. This research was performed with support from National Science Foundation Grant DMR 83-15547.

Registry No. PVB (homopolymer), 25951-54-6; PVC (homopolymer), 9002-86-2; PCIS (homopolymer), 24991-47-7.

References and Notes

- (1) Nagai, K.; Ishikawa, T. *Polym. J. (Tokyo)* **1971**, *2*, 416.
- (2) Doi, M. *Polym. J. (Tokyo)* **1972**, *3*, 252.
- (3) Mattice, W. L.; Carpenter, D. K. *Macromolecules* **1984**, *17*, 625.
- (4) Mattice, W. L.; Carpenter, D. K.; Barkley, M. D.; Kestner, N. R. *Macromolecules* **1985**, *18*, 2236.
- (5) Abe, A.; Jernigan, R. L.; Flory, P. J. *J. Am. Chem. Soc.* **1966**, *88*, 631.
- (6) Mark, J. E. *J. Chem. Phys.* **1972**, *56*, 451.
- (7) Saiz, E.; Riande, E.; Delgado, M. P.; Barrales-Rienda, J. M. *Macromolecules* **1982**, *15*, 1152.
- (8) Yoon, D. Y.; Sundararajan, P. R.; Flory, P. J. *Macromolecules* **1975**, *8*, 776.
- (9) Saiz, E.; Mark, J. E.; Flory, P. J. *Macromolecules* **1977**, *10*, 967.
- (10) Flory, P. J. *Macromolecules* **1974**, *7*, 381.
- (11) Mattice, W. L.; Saiz, E. *J. Polym. Sci., Polym. Phys. Ed.*, in press.
- (12) Mansfield, M. *Macromolecules*, in press.

Dilute Solution Properties of a Polystyrene-Poly(methyl methacrylate) Graft Copolymer Studied by Emission Probe Techniques. 2.¹ Rotational Relaxation Time of the Graft Copolymer by Fluorescence Polarization Measurement

Akira Watanabe² and Minoru Matsuda*

Chemical Research Institute of Non-aqueous Solutions, Tohoku University, Katahira, Sendai, 980 Japan. Received December 3, 1985

ABSTRACT: Dynamic properties of polystyrene (PS)-poly(methyl methacrylate) (PMMA) graft copolymer in dilute solution were studied by means of fluorescence emission probe techniques; a fluorene unit (Fl) is introduced as an energy donor at an appropriate number in the backbone PS chain by copolymerization with 2-vinylfluorene, and a pyrene unit (Py) is introduced as an acceptor at the end of the PMMA chain grafted from Fl. Energy transfer from Fl to Py within the graft copolymer was strongly suggested from the excitation spectra and fluorescence polarized spectra. The micelle formation of PS-PMMA graft copolymer in binary mixed solvents was demonstrated by the effect of polymer chain conformation on the efficiency of the energy transfer from Fl to Py and is discussed on the basis of the data of the rotational relaxation time ρ around the Py located at the end of the grafted PMMA chain; ρ was obtained by the fluorescence polarized spectra and the lifetime of Py. It was revealed that ρ was increased from 10^{-9} to 10^{-7} s, corresponding to the transition phenomena for the formation of the PS-PMMA graft copolymer micelle.

Introduction

Aggregation phenomena of block or graft copolymers in solution have become of interest in recent years because

aggregation processes affect the morphology of the polymer films that are formed from solvent casting.³⁻⁷ Furthermore, block and graft copolymers have the ability to activate a